Atomic Spectroscopy

Article

Data-provenance-aware Stark Broadening Estimation for Automated LIBS Spectral Simulation of Ionic Lines

Yilin Wang,* Toni Aaltonen,* and Shuo Zhang

RoboAI R&D Centre, Satakunta University of Applied Sciences, Pori 28130, Finland

Received: *July 28, 2026;* ***Revised:*** *September 16, 2026;* ***Accepted:*** *September 26, 2026;* ***Available online:*** *September 26, 2026.*

DOI: 10.46770/AS.2026.0075s

ABSTRACT: Laser-induced breakdown spectroscopy (LIBS) simulation requires accurate Stark-width parameters, yet reliable data remain missing for many spectral lines. Current simulators rely mainly on manually maintained tables, simplified analytical formulas, or the STARK-B database — but manual curation is labor-intensive, simplified formulas carry large errors, and STARK-B covers a limited set of lines on a discrete, pre-computed temperature grid. To bridge these gaps, an automated ion-line Stark-width workflow was developed based on the modified semi-empirical (MSE) method on top of the NIST Atomic Spectra Database, with the required oscillator strengths completed through a tiered hierarchy of sources. The MSE formalism is defined for ionized emitters, and the workflow inherits that domain. Each computed width is returned with an uncertainty estimate and a full data-provenance trace, and widths resting on weak inputs are automatically flagged as high-risk. The workflow is accessible through both a web interface and a Python SDK, making Stark widths available at the scale that spectrum-level LIBS applications require. The workflow is validated against two independent references: the semiclassical STARK-B database and the critically evaluated measured widths of Konjević et al. (2002). The MSE formalism itself, applied with hand-curated inputs, carries a stated accuracy of about 50 %; the automated workflow trades part of this precision for coverage, since oscillator strengths are completed from external databases and statistical estimates rather than curated line by line, and sparse level data leave some widths to the approximate lumped term. Within the LIBS-relevant scope of ions II–IV in the optical window, the median ratios of computed to reference widths (W_MSE/W_ref) are 1.15 against STARK-B (802 per-condition comparisons) and 1.05 against the evaluated measurements (1,159 per-condition comparisons). Of these comparisons, 62 % and 58 % respectively fall within a factor of 1.5, and 83 % and 76 % within a factor of two. This provides the basis for obtaining Stark widths at the scale LIBS applications demand, and the identified error sources define clear routes for refining the accuracy. A dedicated treatment of the neutral emitters, the prerequisite for serving a full-spectrum LIBS simulator, is the largest single item of future work.

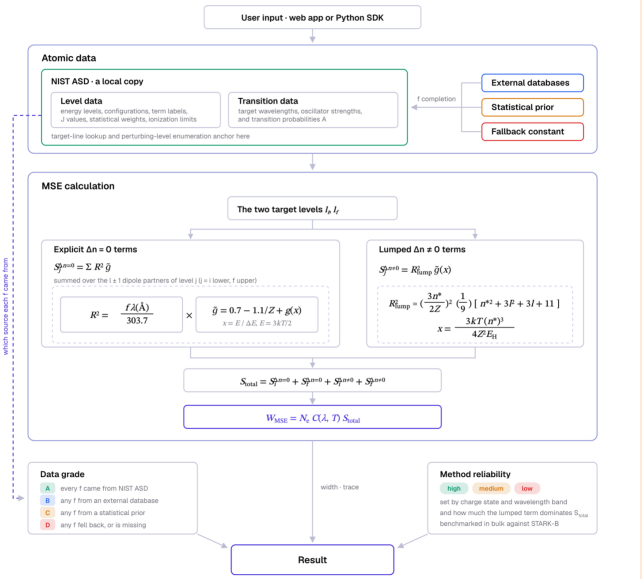

INTRODUCTION

Stark widths are core spectroscopic infrastructure for quantitative laser-induced breakdown spectroscopy (LIBS)[1–3]. As LIBS moves beyond qualitative elemental identification toward calibration-free LIBS[4], synthetic or simulated spectral libraries for model development[5], deconvolution of overlapping features[6], and machine-learning models trained on simulated spectra[7], the shape of individual emission lines becomes a required input rather than a secondary detail. Under typical LIBS plasma conditions, with electron densities of approximately 10^{16}– 10^{18} cm^{-3}, Stark

broadening is often one of the dominant intrinsic broadening mechanisms for atomic and ionic lines[2,8,9]. This is especially important in quantitative studies that use relatively high-resolution spectrometers, or that explicitly deconvolve the instrumental profile[2,6]. Reliable Stark widths are therefore needed both for electron-density diagnostics from measured line widths and for forward modelling of line shapes in synthetic spectra and blended-line analysis[3,8,10]. For electron-density diagnostics a single well-characterised line may suffice, but simulation-based workflows require a width for every line in the modelled range. Broad, accurate Stark-width data are therefore a practical prerequisite for this branch of quantitative LIBS[3,10].

Despite their importance, Stark-width data remain insufficient along two practical axes: transition coverage and condition coverage[11,12]. Accurate experimental compilations[11–13] and semiclassical perturbation (SCP) calculations[14] provide high-value reference data, but they cover only a small fraction of the lines available in modern atomic databases; in our working comparison, the full STARK-B[3] holdings comprise 4,569 distinct transitions, whereas the complete NIST Atomic Spectra Database (ASD)[15] contains 291,639 transitions, so the tabulated reference data cover only about 1.6 % of the transitions listed in the database. The limitation is not only the number of transitions. Even when a line is covered, databases such as STARK-B tabulate widths only on a discrete grid of electron temperatures and densities[3], while quantitative LIBS simulations often require widths at arbitrary plasma conditions. This makes interpolation necessary, and in some workflows density scaling or extrapolation is also required; for uncovered lines, no value can be obtained directly. In addition, at the time of writing, STARK-B provides no public bulk-download facility, which makes large-scale automated use difficult. Some additional Stark-width data are available only in individual papers or printed compilations[11–13], but these sources are also inconvenient for scalable modelling: they usually report widths at a limited set of experimental temperature and density points and using them at other plasma conditions requires extra normalization, interpolation, or recalculation. As a result, practical LIBS modelling is often restricted to a small number of well-studied diagnostic lines and fixed tabulated conditions, which limits scalable quantitative analysis and synthetic-spectrum generation.

For large-scale LIBS modelling, the choice of Stark-width method is a trade-off between physical completeness, data requirements, and automation. The SCP method developed by Sahal-Bréchot and collaborators[14], which underlies STARK-B, provides a rigorous theoretical reference used in this work and is therefore an appropriate accuracy benchmark. However, SCP calculations require a sufficiently complete set of perturbing levels, detailed atomic structure information, and line-specific expert setup, making them difficult to run on demand for many thousands of transitions. In contrast, the semi-empirical[16] and modified semi-empirical (MSE) formulations[17] require only the optically allowed $l \pm 1$ perturbing partners of the two target levels. The MSE formulation is defined for ionized emitters, and this fixes the domain of the present work. The accuracy of the MSE method is about 50 %[3], but its atomic-data requirements are modest and its computational form is tractable. Because the resulting widths are analytic in electron temperature and linear in electron density, the method naturally supports evaluation at arbitrary plasma conditions rather than only at pre-tabulated grid points. The main limitation has not been the formula itself, but its practical use: MSE calculations have historically been carried out line by line, with manual parsing of configurations, manual selection of perturbing levels, and manual collection of oscillator strengths. This makes the method difficult to scale and difficult to reproduce in modern automated LIBS workflows.

Automating the MSE method requires overcoming three practical obstacles. First, the configuration, term, parity, and angular-momentum labels in NIST ASD must be parsed into machine-usable quantum numbers, so that the target transition and its optically allowed perturbing levels can be selected automatically rather than by hand. Second, the required oscillator strengths are incomplete for precisely the transitions the method must sum over. Across all ionization stages only about half of the 76,308 $\Delta n = 0, l \pm 1$ perturbing transitions in ASD lack a usable radiative rate, and stages I–IV, the emitters a LIBS spectrum actually draws on, the gap is wider still: 33,726 of 60,904 (55.4 %) have neither an oscillator strength nor an Einstein (A) coefficient. The range here is I–IV rather than the II–IV over which the method is validated, because the gap being measured is the one LIBS modelling faces as a whole. These missing radiative data must therefore be completed from external databases or estimated from fallback rules before the MSE formula can be applied broadly. Third, the same data gaps introduce an additional uncertainty layer. When a width is produced automatically from a mixture of measured, calculated, externally matched, or estimated atomic inputs, the numerical result alone does not tell the user how much confidence it deserves. Without an explicit record of the data provenance and validation status, users cannot easily judge whether a computed Stark width is reliable for quantitative use or merely a low-confidence extrapolation from incomplete atomic data.

This work does not propose a new theory of Stark broadening, nor does it aim to replace high-accuracy reference calculations. Its goal is to turn the established MSE method into a reproducible, database-driven, and provenance-aware completion pipeline for Stark-width data. By coupling automated width calculation with uncertainty estimation, source tracking, and reliability flagging, it returns not a bare number but a calculation that is transparent about how it was obtained and honest about how far it can be trusted — filling the gap where reference data do not exist, at any plasma condition. In this work, the MSE calculation is automated end to end from NIST ASD level and transition data, so that a Stark width

can be evaluated on demand for a requested spectral line at arbitrary electron temperature and density, rather than only retrieved from a pre-tabulated grid. To address missing radiative inputs, oscillator strengths are completed using external atomic databases such as CHIANTI[18,19], Kurucz[20], and VALD[21] where available, and statistical priors where no direct source exists. The resulting pipeline is validated in two complementary ways: against STARK-B/SCP reference calculations[3], with approximately 802 per-condition comparisons, and against critically evaluated experimental measurements[12], with approximately 1159 per-condition comparisons, with the results stratified by LIBS-relevant emitter families. Each returned width is accompanied by two independent forms of qualification: a reliability grade describing whether the transition lies within the validated method domain, and a data-provenance record describing the origin and confidence level of the atomic inputs used in the calculation. The implementation is delivered both through a web interface and a pip-installable client, returning not only the estimated Stark width but also the full calculation trace behind it, so that every width entering a LIBS model can itself be reproduced and audited.

EXPERIMENTAL

Data sources

Primary structural database: NIST ASD. The primary atomic data source in this work is a local copy of the NIST ASD[15]. NIST ASD provides the target wavelengths, lower and upper energy levels, level configurations, term labels, J values, statistical weights, ionization limits, oscillator strengths, and transition probabilities required by the MSE[17] calculation. All target-line retrieval and perturbing-level enumeration are therefore anchored to the same local ASD database.

External oscillator-strength sources. Because oscillator strengths are incomplete in ASD, additional radiative-data sources were used to supplement missing values. CHIANTI[18,19] and Kurucz[20] data were cross-matched to ASD transitions and stored as local cache files. CHIANTI was used when reliable ion-level matches were available, while Kurucz[20] provided broader coverage through log gf values, which were converted to oscillator strengths. VALD[21]-derived matches were treated as optional cached inputs and were used only when curated match files were available.

Sources evaluated but not adopted as resolution tiers. Several additional sources were explored but were not included as default runtime tiers. Ion-specific literature tables, such as the S II data from Tayal and Zatsarinny[22], were initially considered as dedicated high-priority tiers. However, for the transitions that required oscillator-strength completion, the S II table provided 42 candidate matches, including all 39 CHIANTI matches, and was numerically consistent with the CHIANTI model. Therefore, the maintained, multi-ion CHIANTI database was retained as the curated external tier, while ion-specific literature tables were treated as optional research extensions rather than default runtime sources. OPEN-ADAS[23] ADF04 files were also explored, but reliable level-pair matching did not provide stable production coverage in the current implementation.

Validation references: STARK-B and the Konjević et al. (2002) compilation. Two external references are used exclusively for validation and contribute no input to the width calculation itself. STARK-B, the database of SCP Stark-broadening calculations of Sahal-Bréchot, Dimitrijević and collaborators, provides the theoretical reference[3]; only its SCP entries are retained for benchmarking. The critical compilation of measured Stark widths by Konjević, Lesage, Fuhr and Wiese[12], covering the period 1989–2000, provides the experimental reference; its numerical tables were extracted programmatically, with the extraction and filtering protocol described together with the validation methodology.

MSE Stark-Width Calculation

Method and working formula. Electron-impact Stark widths are computed with the modified semi-empirical (MSE) method[17], which descends from the semi-empirical approach[16] within the impact formulation[24]. The method applies to isolated lines of ionized, non-hydrogenic emitters and carries a stated class accuracy of ±50 %; its decisive practical advantage is that the explicit part of the perturbing-level sum requires only the $l \pm 1$ partners of the two target levels, rather than the complete perturbing-level set demanded by semiclassical calculations. This work follows the formulation restated by Mahmoudi et al.[25], with the Gaunt-factor treatment taken directly from the original[17].

The full width at half maximum, expressed in wavelength units, is assembled as

$$W_{MSE} = N_e \, C(\lambda, T) \, S_{total} \tag{1}$$

where N_e is the electron density and the front factor

$$C(\lambda, T) = \frac{8\pi}{3} \left(\frac{\hbar}{m}\right)^2 \sqrt{\frac{2m}{\pi kT}} \, \frac{\pi}{\sqrt{3}} \, \frac{\lambda^2}{2\pi c} \tag{2}$$

carries all physical constants together with the wavelength and temperature dependence (the factor $\frac{\lambda^2}{2\pi c}$ converts the angular-frequency width of the impact theory to a wavelength width). The dimensionless term sum

$$S_{\text{total}} = S_i^{\Delta n=0} + S_f^{\Delta n=0} + S_i^{\Delta n\neq 0} + S_f^{\Delta n\neq 0} \tag{3}$$

collects, for the initial (i) and final (f) level of the transition, an explicit sum over the $\Delta n = 0$ perturbing levels and a closed form estimate for all $\Delta n \neq 0$ perturbers.

Level parsing and perturber selection. Because the workflow is fully automated, both target levels and all candidate perturbing levels are characterized directly from their ASD configuration and term strings. A dedicated parser extracts the active electron's principal and orbital quantum numbers (n, l), the parent core (including parent-term and seniority labels of multi-electron configurations), the LS term with parity, and J. Perturbing levels for the explicit sum are then selected by the MSE rule: same n and l' = l ± 1, together with, as an additional automation constraint, the same parent core. The core restriction limits the sum to one-electron dipole channels and excludes core-rearrangement (two-electron) transitions, whose matrix elements are not described by the single-jumping-electron picture; it is an engineering choice of the present implementation, not a rule published with the method. Because each perturber enters with a weight scaling as $\frac{1}{\Delta E}$, perturbing levels within 1 cm^{-1} of the target are skipped as quasi-degenerate. This cutoff is a minimal guard against the $\Delta E \to 0$ divergence rather than a treatment of near-degeneracy in general: a perturber a few hundred cm^{-1} away can still dominate the sum and break the isolated-line assumption. All calculations are carried out per line, that is, on J-resolved levels rather than multiplet averages, so the width corresponds to the specific observed wavelength. The two fine-structure components of a doublet are computed as separate lines, each from its own level energies.

Explicit Δn = 0 terms. The explicit part of the sum collects the $l \pm 1$ dipole partners of the two target levels l_i (lower)

$$S_i^{\Delta n=0} = R^2_{l_i,l_{i+1}} \tilde{g}\left(\frac{E}{\Delta E_{l_i,l_{i+1}}}\right) + R^2_{l_i,l_{i-1}} \tilde{g}\left(\frac{E}{\Delta E_{l_i,l_{i-1}}}\right) \quad (4)$$

and l_f (upper)

$$S_f^{\Delta n=0} = R^2_{l_f,l_{f+1}} \tilde{g}\left(\frac{E}{\Delta E_{l_f,l_{f+1}}}\right) + R^2_{l_f,l_{f-1}} \tilde{g}\left(\frac{E}{\Delta E_{l_f,l_{f-1}}}\right) \quad (5)$$

Where $E = \frac{3kT}{2}$ is the kinetic energy of the perturbing electron (k is the Boltzmann constant), and $\Delta E_{l_j,l_{j\pm1}} = |E_{l_j} - E_{l_{j\pm1}}|$ is the energy difference between the levels l_j and $l_{j\pm1}$ $(j = i, f)$; the Gaunt argument is $x = \frac{E}{\Delta E_{l_j,l_{j\pm1}}}$. For each explicit term,

$$R^2_{(l_j,l_{j\pm1})} = \frac{f\,\lambda(\text{Å})}{303.7} \text{ (in units of } a_0{}^2), \quad (6)$$

Where f and λ are the oscillator strength and wavelength of the corresponding $l_j \to l_{j\pm1}$ perturbing transition.

For the Δn = 0 channels of ionized emitters the effective Gaunt factor is the D&K form

$$\tilde{g}(x) = 0.7 - \frac{1.1}{Z} + g(x) \quad (7)$$

at threshold (x ≤ 2, g = 0.20) this reduces to empirical value 0.9 − 1.1/Z (Dimitrijević & Konjević, 1980, **their** Eq. 6) and rises above it as g(x) increases; Z is the spectroscopic charge. The base factor g(x) follows the tabulation given in the same work,

$$g(x) = 0.20\ (x \le 2);\ 0.24, 0.33, 0.56, 0.98, 1.33 \ \ at\ x = 3, 5, 10, 30, 100 \quad (8)$$

interpolated linearly in log x between the tabulated points, and rising monotonically above threshold.

Lumped Δn ≠ 0 terms. The last two terms in Eq. (3), $S_i^{\Delta n\neq0}$ and $S_f^{\Delta n\neq0}$, represent the aggregate contribution of perturbing levels that are not treated in the explicit Δn=0 sum. In the MSE method these terms are not evaluated by enumerating individual Δn≠0 transitions. Instead, each target level $l_j (j = i, f)$ is assigned a closed-form contribution,

$$S_j^{\Delta n\neq0} = R^2_{l_j,\text{lump}} g\left(x_{l_j}^{\Delta n\neq0}\right) \quad (9)$$

The corresponding lumped squared matrix element is

$$R_{l_j,\text{lump}}{}^2 \simeq \left(\frac{3n^*_{l_j}}{2Z}\right)^2 \frac{1}{9}\left[\left(n^*_{l_j}\right)^2 + 3l^2_{l_j} + 3l_{l_j} + 11\right] \quad (10)$$

and the Gaunt argument is

$$x_{l_j}^{\Delta n\neq0} = \frac{3kT\left(n^*_{l_j}\right)^3}{4Z^2E_H} \quad (11)$$

Where k is the Boltzmann constant, $n^*_{l_j} = Z\sqrt{\frac{E_H}{E_{ion}-E_{l_j}}}$ is the effective principal quantum number of target level l_j, l_j is the orbital angular momentum quantum number of its active electron, Z is the spectroscopic charge, and E_H is the hydrogen ionization energy.

Oscillator-strength completion

The coverage problem. Each explicit Δn = 0 term of the width (Eqs. 4–5) requires an oscillator strength: the squared matrix element $R^2(\ell_j, \ell_j \pm 1)$ of every l ± 1 perturbing transition is obtained from its f value through Eq. (6). The calculation is therefore only as complete as the oscillator-strength coverage of the perturbing transitions it must sum over — and for that pool specifically, NIST ASD is markedly incomplete.

Across all ionization stages, ASD[15] holds 76,308 Δn = 0, l ± 1 dipole transitions of the kind the explicit sum draws on. Only 36,325 (47.6 %) carry an evaluated oscillator strength. A further 1,495 (2.0 %) have no tabulated f but do have a transition probability A, from which f is recovered directly. That leaves 38,488 transitions — 50.4 %, about half of the entire perturbing-transition pool. Spectroscopic charge Z counts the neutral atom as 1, so the range Z ≤ 4 accessible to LIBS spans the ionization stages I–IV, and the stages II–IV over which the method is validated correspond to Z = 2–4. Within that range the gap is wider still: 33,726 of 60,904 (55.4 %) transitions carry no radiative rate at all.

Table 1. Oscillator-strength provenance of the 60,904 charge ≤ 4, Δn = 0, l ± 1 dipole transitions

Tier	Transitions	Share
ASD direct	25,998	42.7%
ASD A→f	1,180	1.9%
CHIANTI	748	1.2%
Kurucz gfall	13,126	21.6%
VALD3	129	0.2%
Statistical prior	14,373	23.6%
Fallback(f=0.02)	5,350	8.8%

Table 2. Prior-tier provenance of the 14,373 statistical-prior transitions

Tier	Transitions	Share
Transition-array fit	1,948	13.6%
Multiplet	251	1.7%
Transition-array average	3,420	23.8%
l-bucket	7,307	50.8%
Charge-stage pool	1,447	10.1%

The resolution ladder. Each perturbing transition that lacks an ASD oscillator strength is completed by descending a fixed, provenance-ranked ladder and taking the first source that covers it, so every value comes from the most direct source available:

- ASD direct — the evaluated oscillator strength in NIST ASD, when present.
- ASD A → f — otherwise, if ASD lists a transition probability A, f is recovered from $f = 1.49919 \times 10^{-16} \lambda^2(\text{Å}) (g_u/g_l) A$, keeping the value within the same evaluated source.
- CHIANTI[18,19] — the curated CHIANTI model; the highest-quality external database.
- Kurucz gfall[20] — the broad, largely semi-empirical Kurucz line list; the wide-coverage tier.
- VALD3[21] — for the few ions still uncovered (in practice only Th II).
- Statistical priors — where no database covers the transition, f is estimated from the same ion's known oscillator strengths (Section 3.3).
- Flat fallback f = 0.02 — a flagged last resort that keeps the perturber in the explicit sum instead of dropping it (Section 3.4).

External matches (CHIANTI, Kurucz gfall and VALD3) are accepted only when both ASD levels of a transition map onto the source's levels by configuration, term, and J (with an energy-tolerance guard); they are harvested offline and frozen into versioned caches, so runtime resolution is a local lookup with no network dependence, while the statistical priors are fitted at run time from the same ion's ASD pool. Applied to the 60,904 charge ≤ 4, Δn = 0 perturbing transitions of Section 3.1, the ladder resolves them as follows.

Grouped by provenance, 44.6 % rest on evaluated ASD data, 23.0 % on external databases, 23.6 % on statistical priors, and 8.8 % on the flat fallback.

The matching behind Table 1 and the STARK-B pairing of Section 4.2 was verified line by line against the configuration and term labels of both levels: VALD3 (100 %), a deterministic sample of the CHIANTI (32 %) and Kurucz (5 %) level-pair matches, and every STARK-B pairing confirmed within the narrow window of the benchmark ladder (100 %). No pairing was found to connect different levels.

Statistical priors. Perturbing transitions that no database covers are estimated from the statistical behavior of the same ion's own oscillator strengths, through a fixed hierarchy of estimators, each tried in turn until a pool holds at least three known values:

1) Transition-array fit — a scaled fit within the same transition array, following the systematic oscillator-strength trend across the array.
2) Multiplet — the known f-values of the same multiplet.
3) Transition-array average— the same, pooled at the transition-array level.
4) l-bucket — the same ion's transitions sharing the active electron's orbital angular momentum l.
5) Charge-stage pool — the broadest, ion-wide pool.

Within the multiplet and transition-array tiers the pooling is performed on the reduced line strength rather than on f directly — a quantity that varies far less across a multiplet — and the result is converted back to an oscillator strength, so the estimate respects the physical trend of the array instead of averaging dissimilar lines; the broader tiers take the robust central value of their pool. If no tier qualifies, the transition falls to the flat fallback.

Of these 14,373 prior-resolved transitions (Table 2), the broad l-bucket pool supplies half (7,307; 50.8 %), the transition-array tiers (fit and average) a further 37 % (5,368), the ion-wide charge-stage pool 10 % (1,447), and the narrow multiplet tier only 1.7 % (251) — the specific tiers resolve what they can, and the l-bucket carries the majority.

Fallback and bias control. A perturbing transition that no tier of the ladder resolves is assigned a flat oscillator strength f = 0.02 rather than being dropped. Dropping a perturber is not a neutral omission: its weight passes to the lumped $\Delta n \neq 0$ approximation, which systematically underestimates the width. A crude but flagged explicit term is therefore preferable to a silent one; 5,350 of the charge ≤ 4 transitions (8.8 %) rest on this fallback.

Two safeguards keep the completion honest. Every value carries its provenance through to the final result, so the reliability grade can down-weight any width whose explicit sum leans on fallback or prior estimates, and a fallback-heavy width is never returned

without warning. More decisively, stratifying the benchmark by oscillator-strength provenance reveals no systematic offset between widths built purely on evaluated ASD data and those built on completed values: the completion extends coverage without biasing the physics — which is what licenses its use at scale.

Uncertainty estimate. Every oscillator strength entering the calculation is carried as a nominal value together with a lower and an upper bound, and these bounds propagate to a band on the reported width. Where the value is taken from the local ASD copy, whether given directly or converted from the transition probability, the two bounds coincide with the nominal value and the band contributed is of zero width. Where an external database supplies the value, the bounds are those the source provides and collapse to the value itself where it provides none. Where a statistical prior supplies the value, the nominal is the median of the comparable transitions drawn on and the bounds are the tenth and ninetieth percentiles of that same sample, so the width of the bracket reports the spread of the population the estimate was taken from. Where no sample reaches the minimum size and the flat default is used, the value is assigned a deliberately wide factor-of-five bracket.

The explicit contribution of a perturbing level is proportional to its oscillator strength, and the Gaunt factor is evaluated once at the nominal level separation and temperature, so each perturbing term inherits its own f bracket unchanged. The two ends of the explicit sum are then formed by summing every term at its lower bound and again at its upper bound. The lumped $\Delta n \neq 0$ term enters both ends at its single value, since it consumes no oscillator strength. The width being linear in the dimensionless term sum, the reported band is that sum's band scaled by the same prefactor.

Two properties of the band require care in interpretation. It is a worst-case envelope rather than a statistical propagation: the lower end assumes every completed oscillator strength sits simultaneously at its lower bound, no correlation between perturbing transitions is modelled, and no quadrature is taken. It is also a measure of oscillator-strength provenance alone. It excludes the intrinsic uncertainty of the semiclassical formalism, and it excludes the lumped term, which is the branch responsible for the largest systematic deviation identified below. A line whose explicit sum draws entirely on the local ASD copy therefore reports a band of zero width while still carrying the full uncertainty of the formalism, and a narrow band must not be read as an accurate width. The band answers one question only, which is how far the completed input data could have moved the result. It should be interpreted as a provenance-aware sensitivity range rather than a complete physical uncertainty interval for the MSE model.

Validation methodology

Scope and metrics. Two external references, introduced among the data sources above, anchor the validation. STARK-B[3] supplies the theoretical reference: SCP calculations with a stated accuracy of 20–30 %, resting on a more rigorous treatment and on different atomic inputs than the semi-empirical formula under test. The critical compilation of Konjević, Lesage, Fuhr and Wiese[12] supplies the experimental reference: measured Stark widths whose uncertainties the reviewers grade explicitly, on a combined-uncertainty (rss) scale running from class A (within 15 %) to class D (beyond 50 %). The two references fail in different ways. The first carries the model error of an independent theory; the second carries graded experimental uncertainty from plasma diagnostics and profile fitting. Agreement demonstrated against both therefore cannot be an artefact of tuning to either source, and concordance between the two benchmarks is itself part of the evidence.

The validation scope is declared before any ratio is examined, and it is set by the application[1,26]. LIBS practice targets specific emitter families: light elements (C, N, O, B, P), rock-forming elements (Si, Al, Ca, Na, Mg, K, Ti), alloy constituents (Fe, Ni, Cu, Zn, Sn, Cr, Mn, Be), battery metals (Li, Co), the rare-earth family (represented by Sc in the present reference sets), environmental heavy metals (Pb, Cd, Hg), the halogens together with sulfur (F, Cl, Br, I, S), and the buffer gases (He, Ne, Ar) that form the plasma environment in gas-controlled LIBS setups. Species that appear in the reference sets but fall outside these families (Kr, Xe, In, Ba) are computed and reported separately rather than silently dropped, and all-element statistics accompany the scoped ones throughout. The primary scope further restricts the comparison to ions II–IV in the optical window 2000–9000 Å; neutral-atom rows are retained only as out-of-domain evidence, the MSE formulation being stated for ionized emitters. On the experimental side the primary scope keeps width grades A and B, with B^+ counted in class B. On the theoretical side it keeps grid temperatures at or below 50 000 K, since the STARK-B grids extend to 10^6 K, far beyond LIBS conditions. The reference conditions themselves cover the LIBS regime: the measured widths retained in the primary scope were obtained at electron densities of 1×10^{16} to 2.7×10^{18} cm^{-3} and temperatures of 6,500 to 130,000 K. The validation thus compares computed widths with reference widths at the reference conditions; an end-to-end test on a LIBS plasma, in which computed widths are used to recover the electron density from measured profiles, remains to be made.

Agreement is quantified line by line as the ratio W_MSE/W_ref, both widths being full widths at half maximum, and summarised by the median ratio together with the fractions of comparisons falling within factors of 1.5, 2, and 3. These ratio statistics follow the form in which the accuracy of the method was originally established: the founding comparison assessed ratios of measured to calculated widths, from which the commonly quoted accuracy of about ±50 % derives, so the present results read on the same scale as the original accuracy statement. The three figures quoted in this work are nevertheless distinct quantities. The ±50 % is the class accuracy of the formalism as originally established, a bound

on the deviation of individual widths; the median ratio measures the systematic bias of the estimator over a population; and the fraction within a factor of two measures the scatter of individual widths about that bias. A median within 15 % of unity therefore does not mean that individual widths are accurate to 15 %.

Benchmark against STARK-B. From the 159,170 tabulated STARK-B rows, only entries sharing the domain and observable of the present method are retained: widths computed with the SCP method for electron impact (ion-perturber entries are excluded), emitters of spectroscopic charge ≤ 4, and wavelengths inside the optical window. Entries computed with the MSE method itself, which STARK-B also holds for some ions, are likewise excluded, so that the benchmark tests accuracy against an independent theory rather than self-consistency. Deduplicated across the temperature–density grid, the selection leaves 1165 distinct transitions, of which 1096 carry levels classifiable in LS coupling; the remainder are jK- or bracket-coupled and cannot be confirmed against ASD terms. This deduplicated list serves only the coverage census; the ratio benchmark itself is built per condition, as described below.

Each reference transition must be paired with its ASD counterpart before its width can be recomputed. The STARK-B levels are parsed into principal and orbital quantum numbers, LS term, parity and J, and an ASD line is accepted only when both of its levels agree in n and l, term and parity, and in J where STARK-B resolves it. This J-resolved confirmation prevents pairing a reference transition with a neighbouring line that shares its wavelength but not its structure. Because STARK-B quotes theoretical or multiplet-mean wavelengths, which can lie tens of Å from the observed line, the search for the counterpart runs a widening window ladder of ±2–5, ±30 and ±80 Å; correctness is enforced at every step by the level confirmation, never by wavelength proximity. The ladder confirms 500 transition pairs spanning ionization stages I–IV, 98 of them beyond the narrow window, including the Ca II resonance doublet and Al III and Si IV lines that quote multiplet-mean wavelengths.

For the ratio benchmark, each confirmed transition is expanded back to its full STARK-B temperature grid, mirroring the per-measurement design of the experimental benchmark. At each grid temperature a single density point is kept, the one nearest 10^{17} cm^{-3}: both sides scale linearly with electron density in the LIBS range, the MSE width by construction and the SCP tabulations to a demonstrated log–log slope of 1.00 below 10^{18} cm^{-3}, so additional density rows would duplicate rather than inform. The expansion yields 2 815 per-condition comparisons, and W_MSE is recomputed at the exact temperature and density of each retained point. The a priori scope defined above reduces these to 802 comparisons over ions II–IV of the LIBS emitter families at temperatures up to 50 000 K. Per-transition medians are reported alongside the per-condition statistics as a check that the varying grid sizes, from 3 to 86 points per transition, do not drive the result. The ratio is then examined along the axes the method's structure predicts should matter, ionization stage, temperature, oscillator-strength provenance and emitter family, with the results reported in the following section.

Benchmark against measured widths. The experimental reference is the critical compilation of Konjević, Lesage, Fuhr and Wiese[12] which reviews measured Stark widths and shifts of neutral and ionized atoms over the period 1989–2000. Its numerical tables were parsed programmatically, retaining every tabulated plasma condition and accuracy grade as one record per measured transition at a given electron temperature and density. The raw extraction holds 2522 rows spanning 77 spectra, each carrying the spectrum, transition array, multiplet, wavelength, temperature, electron density, measured full width at half maximum, measured shift, accuracy grade and literature reference; table notation, including bracket-coupled multiplet labels and prime marks in transition arrays, was normalised during extraction.

Only rows defining a single recomputation point are retained. Shift-only rows provide no width and are excluded; rows quoting the width as a range, and rows quoting the electron density as a range or as a differential entry, define no single condition and are excluded as well. Temperature ranges are kept at their midpoint and flagged as range-derived. Four table misprints, each verified against the neighbouring members of the same multiplet, are corrected before computation. These filters leave 2395 of the 2522 extracted rows computable.

Each experimental line is then paired with its ASD counterpart through the emitting element, ionization stage and tabulated wavelength, using a 2 Å search window and the same same-core line selection the workflow applies in production. Rows without a classifiable ASD match are retained in the coverage audit but excluded from the ratio statistics; these are dominated by multiplet-mean wavelengths lying too far from any individual ASD component, and by levels lacking sufficient identification for automated processing. MSE widths are obtained for 2230 rows, representing 1327 distinct experimental lines; 165 computable rows, from 121 distinct lines, find no classifiable match.

For every matched row, W_MSE is recomputed at the row's own electron temperature and density, midpoints entering only through the flagged range rows described above, and compared as the ratio W_MSE / W_exp. The a priori scope defined above reduces the computed set to 1159 rows over ions II–IV of the LIBS emitter families with width grades A and B. These 1159 rows correspond to 575 distinct spectral lines, each line contributing one row per tabulated temperature–density condition. The ratio is then examined by ionization stage, experimental grade, temperature, electron density, emitter family and identifiable outlier classes, with the results reported in the following section.

Availability (Frontend &Python SDK). The completed Stark-width pipeline is made available through both an interactive web interface and a Python software development kit (SDK). The web interface (https://libs.roboai.fi/stark), hosted at the endpoint of the project frontend, is intended for direct inspection of individual lines: users can specify the emitting species, wavelength or transition, electron temperature, and electron density, and receive the computed Stark width together with the matched atomic levels, perturbing transitions, oscillator-strength sources, reliability grade, and calculation trace. For programmatic use, the Python SDK (https://pypi.org/project/roboai-stark-client/) exposes the same calculation workflow through a lightweight client interface, enabling batch requests from LIBS simulations, synthetic-spectrum generators, and data-analysis pipelines. Both access routes call the same backend calculation engine and therefore return consistent widths, provenance metadata, and quality flags. –The availability of both modes is intended to support two complementary use cases: manual expert review of individual calculations through the frontend, and reproducible large-scale completion of Stark-width data through Python scripts (Fig. 1).

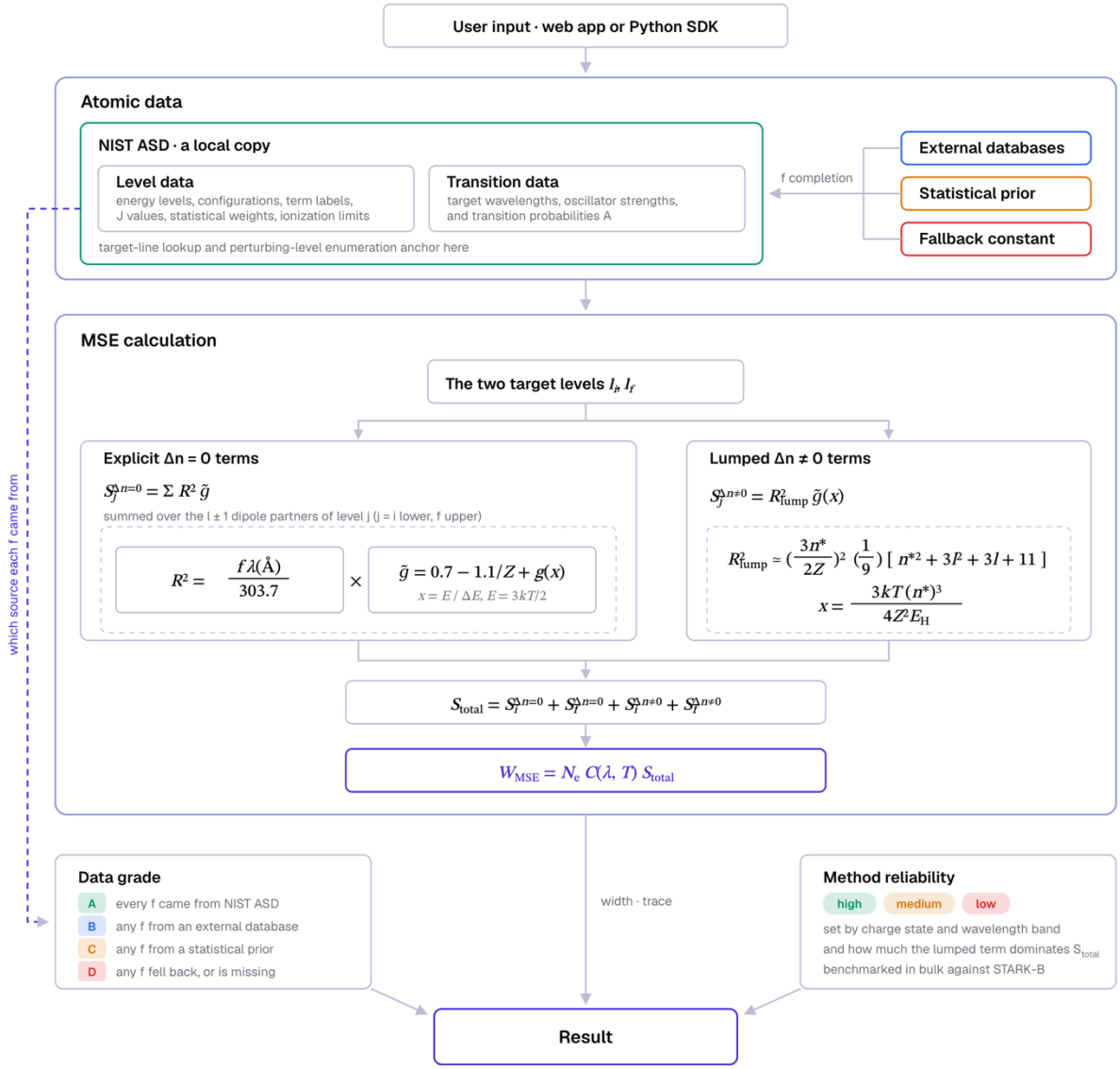

Fig. 1 Provenance and workflow of a single MSE width. The local NIST ASD copy supplies the level data and the transition data, and anchors both target-line lookup and perturbing-level enumeration. Where it carries no oscillator strength for a required Δn = 0 partner, the f-completion step supplies one from an external database, a same-ion statistical prior, or a flat default, in that order of priority. The calculation then splits into the explicit Δn = 0 sum, which consumes one oscillator strength per dipole partner, and the closed-form lumped Δn ≠ 0 term, which consumes none; the two combine into S_total and thence into W_MSE.

RESULTS AND DISCUSSION

Across the LIBS-relevant ionization stages the automated MSE widths agree with both independent references to within a factor of two for the large majority of lines. Against the STARK-B semiclassical-perturbation calculations the median ratio W_MSE/W_ref is 1.15, and against the critically evaluated measured widths it is 1.05, so the systematic bias of the estimator is within 15 % of either reference; the scatter about that bias places 83 % and 76 % of comparisons within a factor of two (Table 3). The two references carry independent error budgets, one purely theoretical and one experimental, so their concurrence shows that the agreement is a property of the estimator rather than of any single dataset.

The largest identifiable error source is tied to the lumped Δn≠0 term of the width. Every MSE width is the sum of an explicit Δn=0 contribution, which requires an oscillator strength for each perturbing transition, and a data-free closed-form lumped term that stands in for the remaining perturbers. When the lumped term carries more than half of the total the accuracy falls monotonically, from about 85 % within a factor of two at low lumped share to roughly 15 % once the lumped share exceeds three quarters, and the failure is directional: these widths systematically underestimate, because the explicit sum has starved and the crude lumped estimate that replaces it is too small (Fig. 2). The starvation itself traces to the level tables rather than to the oscillator strengths: for many of these emitters the required perturbing levels are simply absent from NIST. The Al III line at 2907 Å is representative: its upper level 6g couples most strongly to 6h, a level NIST does not hold at all, and a missing level never enters the sum, nor can it be flagged by the f-value provenance, which sees only whether an existing line lacks its oscillator strength, not whether an entire level is absent. Supplementing such missing high-l levels through hydrogenic approximations, so that the explicit sum can be completed where the tables end, is the planned remedy for this class.

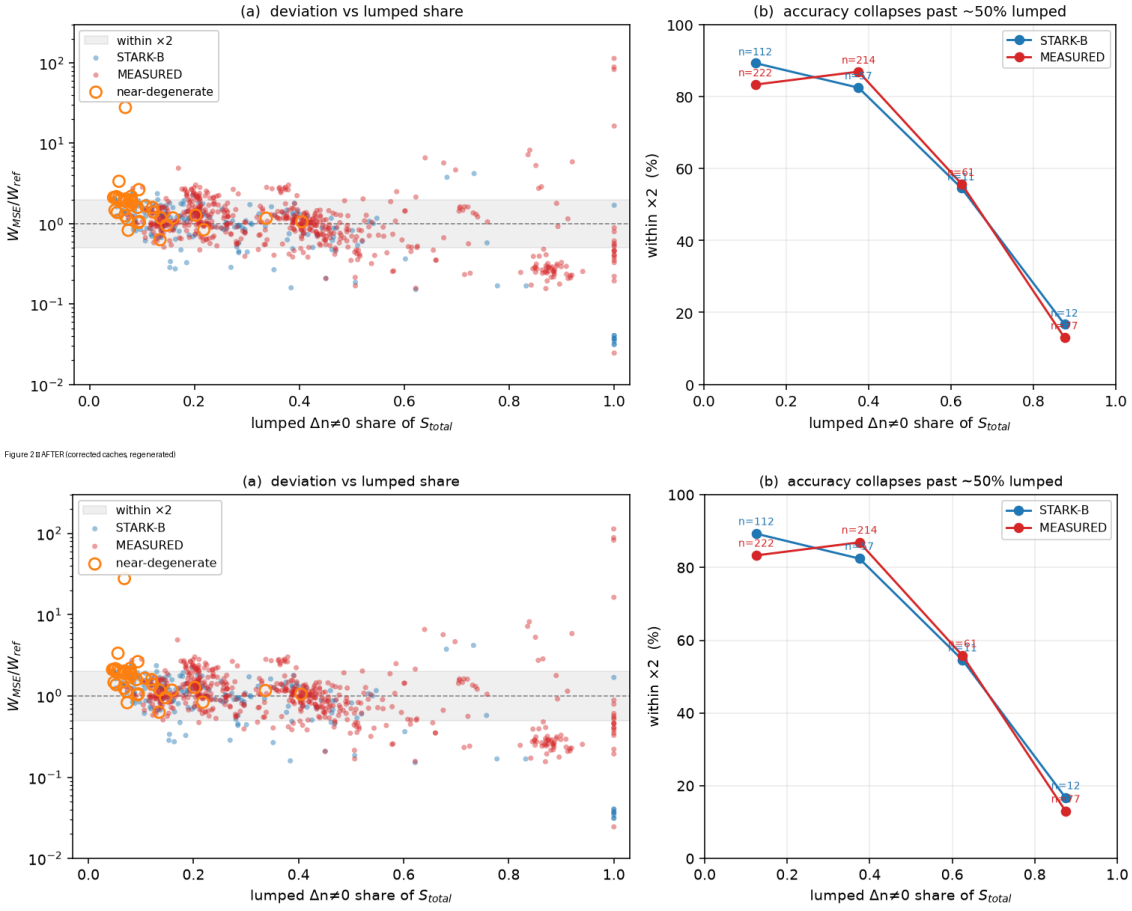

Fig. 2 Deviation from the two references as a function of the lumped Δn≠0 share of S_total, for LIBS-relevant ions II–IV. (a) Per-transition ratio W_MSE/W_ref against both references; the shaded band marks agreement within a factor of two, and the open orange markers are the near-degenerate class discussed below, which sit at low lumped share yet scatter upward. (b) Fraction of transitions within a factor of two per lumped-share bin: accuracy holds near 85 % below a lumped share of about one half and collapses to roughly 15 % above three quarters, with the two independent references tracing the same curve.

Table 3. Overall agreement of the MSE widths against the two references, for LIBS-relevant ions II–IV

Reference	n	Median W_MSE/W_ref	Within ×1.5	Within ×2	Within ×3
STARK-B SCP (theory)	802	1.15	62%	83%	93%
Measured widths (Konjević 2002)	1159	1.05	58%	76%	92%

Table 4. Ablation of the f-value completion ladder (median W_MSE/W_ref / within ×2)

Group	Ladder ON	Ladder OFF
STARK-B (all ladder-using conditions, n=189)	0.93 / 83%	0.77 / 79%
MEASURED (all ladder-using conditions, n=440)	1.15 / 75%	1.05 / 67%
NIST + external DB (n=488)	1.05 / 75%	1.02 / 68%
contains fallback (n=18)	0.67 / 56%	0.50 / 50%
contains stat. prior (n=123)	1.19 / 93%	0.78 / 83%

A second contribution comes from the oscillator-strength input to the explicit Δn=0 term itself, which is only as accurate as the f-values available to it. Where the evaluated database lacks a required value the completion scheme supplies one, and the estimate inherits the reliability of its source: about one third of the LIBS-scope lines draw part of their explicit sum from external databases or statistical priors rather than from evaluated data, and each carries the added uncertainty of its source into the width. A smaller remainder, roughly 3 % of lines, exhausts every source and falls back to a flat default value; that deliberately conservative default sits below the true oscillator strength, suppresses the explicit sum, and produces a directional under-estimation with ratios centred near 0.5, so these lines overlap the lumped-dominated tail while differing from it in origin, a genuine data gap rather than a structural one. The Δn=0 term is therefore accurate only to the extent that its oscillator strengths are, and this input dependence is a real error source distinct from the formalism itself.

The provenance record ranks the sources by their intrinsic reliability, evaluated ASD values first, then the external databases, then the statistical priors, then the flat fallback, and a width is characterised by the weakest source that entered its explicit sum. That ranking is not fitted to the benchmark, and the benchmark does not rank the tiers. Grouped by weakest source, the comparisons with measured widths give medians of 1.04, 1.14, 1.23 and 0.46 for widths resting entirely on evaluated ASD values and for those whose weakest source is an external database, a statistical prior and the flat fallback respectively, with 77 %, 73 %, 93 % and 38 % of comparisons within a factor of two and central 80 % intervals of 0.51–2.21, 0.50–2.22, 0.70–1.64 and 0.24–0.98 (n = 698, 361, 71 and 29). The apparent tightness of the statistical-prior group does not mean that a prior is as reliable as an evaluated value. That group is 6 % of the benchmark, drawn from six ions, and in those widths the prior supplies a median of 4 % of the explicit sum, three quarters of them below 14 %, the remainder still coming from evaluated data; in the ten comparisons where the prior supplies more than a quarter of the sum, all Ar III–IV, the median falls to 0.71. The same caution applies to the external-database group, where the external value carries 3 % or less of the sum in three quarters of the widths. What the stratification does establish is the other end of the ladder: the widths that contain a fallback value, or a perturber for which no line exists at all, are the under-estimated class already described, at half the reference and almost never above it. A fallback in the provenance record is therefore to be read as a warning, whereas an external or prior source marks the ancestry of a value whose expected accuracy is carried by the method reliability class.

That the completion scheme is a working part of the accuracy, and not merely a neutral substitution, is demonstrated by an ablation (Table 4). In the ladder-on configuration the explicit sum draws on the full completion: evaluated NIST oscillator strengths supplemented by the external databases and the statistical priors. In the ladder-off configuration these supplements are removed, so only the evaluated NIST values remain and every perturbing transition NIST cannot supply falls to the flat default of f = 0.02. Recomputed under both configurations, the 629 benchmark conditions whose transitions draw any oscillator strength from the completion lose four to eight points within a factor of two against the two references (from 83 to 79 % and from 75 to 67 %); conditions whose perturbers are fully covered by evaluated NIST values are identical in the two runs by construction and are therefore excluded. The statistical-prior tier shows the effect most clearly, its median over the two references moving from 1.19 with the completion to 0.78 without it, from slightly high into systematic under-estimation. At present evaluated and external sources resolve about two thirds of the perturbing transitions, statistical priors a further quarter, and the flat fallback the remaining tenth; sharpening the priors and algorithmically shrinking the fallback tier is therefore a direct route to accuracy, not merely to coverage.

A third, rarer contribution acts in the opposite direction and is orthogonal to both the lumped and the oscillator-strength mechanisms. A small class of lines is dominated by a single near-degenerate perturber: when a perturbing level lies only a few hundred cm^{-1} from the emitting level its $1/\Delta E$ weight inflates the explicit sum by one to two orders of magnitude and the width is

over-estimated, the Si II 4621 Å line being the clearest example. Because such lines carry a low lumped share and a complete set of oscillator strengths, the over-estimate is a numerical-sensitivity effect rather than a data gap, and it appears as the upward-scattering open markers at low lumped share in Fig. 2a, marked wherever a single perturbing level closer than 1000 cm^{-1} supplies more than 40 % of the explicit sum. Future work will promote this criterion to a sensitivity flag returned with the width.

The workflow also carries a limitation inherent to the method itself. Most transitions in a LIBS spectrum belong to neutral atoms, and for these the method fails in a qualitatively different way from any of the ionic error classes, with both references in agreement: neutral widths scatter over two orders of magnitude, with only 35 % and 60 % within a factor of two against STARK-B and the measured compilation respectively. The failure originates in the formalism, which is defined for charged emitters, and every neutral result is accordingly flagged as out of domain by the workflow. Crossing this boundary requires a dedicated treatment for neutral emitters and is the largest single item of future work.

These error sources are condensed into method reliability class returned with every width, which takes one of three values, high, medium or low, and is assigned in two steps. A base class follows the ionization stage, taking its values from the benchmark resolved by charge: stages II and III, on which agreement is closest, are rated high; stage IV, which benchmarks systematically low, is rated medium; the neutral stage, together with stages beyond the benchmarked range, is rated low on the formal grounds set out above. A single per-line test then acts on the composition of the width itself: where the lumped $\Delta n \neq 0$ term supplies half or more of the dimensionless term sum, the line is marked lumped-dominated and the class drops one step, the threshold following the accuracy behaviour of Fig. 2b.

CONCLUSION

An automated Modified Semi-Empirical estimator has been developed that combines the NIST Atomic Spectra Database with a layered oscillator-strength completion scheme to deliver Stark widths for LIBS-relevant ion lines together with a per-line data-provenance grade. The validated domain is the ionized emitters; for the neutral atoms that also populate LIBS spectra the formalism does not apply, and a dedicated treatment for them remains the largest single item of future work. Benchmarked against two references with independent error budgets, the STARK-B semiclassical-perturbation calculations and the critically evaluated measured widths of the 2002 Konjević compilation, the estimator reproduces both to a median within 15 % and places three quarters to four fifths of all singly-to-triply-ionized optical lines within a factor of two. The agreement of two independent references establishes this accuracy as a property of the method rather than of any single dataset. The residual deviation is not diffuse but resolves into identifiable contributions: a systematic under-estimation confined to ion lines whose width falls to the data-free lumped $\Delta n \neq 0$ term, rooted in perturbing levels absent from the NIST tables; an input dependence on the completed oscillator strengths, for which an ablation shows the completion scheme to purchase measurable accuracy rather than mere coverage; and a rarer over-estimation of ion lines dominated by a single near-degenerate perturber. The validated domain is the ionized emitters: for the neutral atoms that dominate LIBS spectra the formalism does not apply, and a dedicated treatment for them remains the largest single item of future work. The estimator therefore does not yet reach reference-grade precision, but it attains a level fit for practical use while doing what tabulated width compilations cannot: every value is accompanied by a full account of where its error originates and by an explicit, inspectable record of how it was computed, from each perturbing transition and its oscillator-strength source down to the split between the explicit and lumped terms. Exposed through a web interface and a Python SDK, it turns Stark-width estimation from a hand-curated, line-by-line exercise into an operation that can be run at the scale a full LIBS spectrum demands. This makes it practical to incorporate Stark broadening into synthetic LIBS spectra as a routine ingredient rather than one neglected or crudely approximated.

AUTHOR INFORMATION

Yilin Wang works as a researcher at the RoboAI Research Centre, Satakunta University of Applied Sciences, Finland. Her work focuses on web-based simulation services for Optical Emission Spectroscopy (OES) and Laser-Induced Breakdown Spectroscopy (LIBS), combining plasma spectroscopy, physics-based modelling, and artificial intelligence for spectral prediction and analysis.

Toni Aaltonen works as a Senior Researching Lecturer at the RoboAI Research Centre, Satakunta University of Applied Sciences, Finland. His research focuses on laser-induced breakdown spectroscopy, optical emission spectroscopy, plasma diagnostics, and machine-learning methods for spectroscopic analysis. His current work includes, synthetic spectrum generation, physics-guided data augmentation, and realistic validation of machine-learning models. He was also a member of the founding teaching team for Finland's first bachelor's degree programme dedicated to artificial intelligence.

Corresponding author

* Y. L. Wang

Email address: yilin.wang@samk.fi

* T. Aaltonen

Email address: toni.aaltonen@samk.fi

Notes

The authors declare no competing financial interest.

ACKNOWLEDGMENTS

The work was carried out within the ROSS (Raskasmetallien online spektroskopia Satakunnassa) project at Satakunta University of Applied Sciences (SAMK), which aims to develop real-time online monitoring systems for heavy metal emissions in industrial processes using optical emission spectroscopy and AI-based analytics. The project is co-funded by the European Union Just Transition Fund (JTF) and SAMK.

REFERENCES

1. Hahn, D. W., and Omenetto, N. Laser-induced breakdown spectroscopy (LIBS), part II: Review of instrumental and methodological approaches to material analysis and applications to different fields. *Appl. Spectrosc.*, 2012, **66**, 347–419. https://doi.org/10.1366/0003702128404684
2. Thomas, J., and Joshi, H. C. Review on laser induced breakdown spectroscopy: Methodology and technical developments. *Appl. Spectrosc. Rev.*, 2023, **59**, 124–155. https://doi.org/10.1080/05704928.2022.2156137
3. Sahal-Bréchot, S., Dimitrijević, M. S., Moreau, N., and Ben Nessib, N. The STARK-B database as a resource for "STARK" widths and shifts data: State of advancement and program of development. *Adv. Space Res.*, 2014, **54**, 1148–1151. https://doi.org/10.1016/j.asr.2014.06.014
4. Ciucci, A., Corsi, M., Palleschi, V., Salvetti, A., and Tognoni, E. New procedure for quantitative elemental analysis by laser-induced plasma spectroscopy. *Appl. Spectrosc.*, 1999, **53**, 960–964. https://doi.org/10.1366/0003702994987615
5. Jahoda, P., Porizka, P., and Prochazka, D. Machine learning for recognizing minerals from multispectral data. *Analyst*, 2021, **146**, 184–195. https://doi.org/10.1039/D0AN01488A
6. Liu, K., Wang, X., Zhang, Y., and Li, Z. Interference correction for laser-induced breakdown spectroscopy using a deconvolution algorithm. *J. Anal. At. Spectrom.*, 2020, **35**, 762–766. https://doi.org/10.1039/C9JA00387A
7. Huang, Y., Harilal, S. S., Bais, A., and Hussein, A. E. Progress toward machine learning methodologies for laser-induced breakdown spectroscopy with an emphasis on soil analysis. *IEEE Trans. Plasma Sci.*, 2023, **51**, 1729–1749. https://doi.org/10.1109/TPS.2023.3241217
8. Aragón, C., and Aguilera, J. A. Characterization of laser induced plasmas by optical emission spectroscopy: A review of experiments and methods. *Spectrochim. Acta B*, 2008, **63**, 893–916. https://doi.org/10.1016/j.sab.2008.05.009
9. Geethika, B. R., Thomas, J., Rajesh, R. K., Dave, J., and Joshi, H. C. Effect of polarization on spectroscopic characterization of laser produced aluminium plasma. *Spectrochim. Acta B*, 2024, **221**, 106985. https://doi.org/10.1016/j.sab.2024.106985
10. Gigosos, M. A. Stark broadening models for plasma diagnostics. *J. Phys. D Appl. Phys.*, 2014, **47**, 343001. https://doi.org/10.1088/0022-3727/47/34/343001
11. Konjević, N. Plasma broadening and shifting of non-hydrogenic spectral lines: present status and applications. *Phys. Rep.*, 1999, **316**, 339–401. https://doi.org/10.1016/S0370-1573(99)00032-0
12. Konjević, N., Lesage, A., Fuhr, J. R., and Wiese, W. L. Experimental Stark widths and shifts for spectral lines of neutral and ionized atoms (A critical review of selected data for the period 1989 through 2000). *J. Phys. Chem. Ref. Data*, 2002, **31**, 819–927. https://doi.org/10.1063/1.1483367
13. Lesage, A. Experimental Stark widths and shifts for spectral lines of neutral and ionized atoms: A critical review of selected data for the period 2001–2007. *New Astron. Rev.*, 2009, **52**, 471–535. https://doi.org/10.1016/j.newar.2009.09.001
14. Sahal-Bréchot, S., Dimitrijević, M. S., and Ben Nessib, N. Widths and shifts of isolated lines of neutral and ionized atoms perturbed by collisions with electrons and ions: An outline of the semiclassical perturbation (SCP) method and of the approximations used for the calculations. *Atoms*, 2014, **2**, 225–252. https://doi.org/10.3390/atoms2020225
15. NIST. Atomic Spectra Database. *NIST*, 2021. https://doi.org/10.18434/T4W30F
16. Griem, H. R. Semiempirical formulas for the electron-impact widths and shifts of isolated ion lines in plasmas. *Phys. Rev.*, 1968, **165**, 258–266. https://doi.org/10.1103/PhysRev.165.258
17. Dimitrijević, M. S., and Konjević, N. Stark widths of doubly- and triply-ionized atom lines. *J. Quant. Spectrosc. Radiat. Transf.*, 1980, **24**, 451–459. https://doi.org/10.1016/0022-4073(80)90066-6
18. Dere, K. P., Landi, E., Mason, H. E., Monsignori Fossi, B. C., and Young, P. R. CHIANTI - an atomic database for emission lines - I. Wavelengths greater than 50 Å. *Astron. Astrophys. Suppl. Ser.*, 1997, **125**, 149–173. https://doi.org/10.1051/aas:1997219
19. Del Zanna, G., Dere, K. P., Young, P. R., and Landi, E. CHIANTI—An Atomic Database for Emission Lines. XVI. Version 10, Further Extensions. *Astrophys. J.*, 2021, **909**, 38. https://doi.org/10.3847/1538-4357/abd8ce
20. Kurucz, R. L. Including all the lines: data releases for spectra and opacities. *Can. J. Phys.*, 2017, **95**, 825–827. https://doi.org/10.1139/cjp-2016-0794
21. Ryabchikova, T., Piskunov, N., Kurucz, R. L., Stempels, H. C., Barklem, P. S., and Weiss, A. A major upgrade of the VALD database. *Phys. Scr.*, 2015, **90**, 054005. https://doi.org/10.1088/0031-8949/90/5/054005
22. Tayal, S. S., and Zatsarinny, O. Breit–Pauli transition probabilities and electron excitation collision strengths for singly ionized sulfur. *Astrophys. J. Suppl. Ser.*, 2010, **188**, 32. https://doi.org/10.1088/0067-0049/188/1/32
23. Summers, H. P. The ADAS User Manual, version 2.6. 2004. https://www.adas.ac.uk/manual.php
24. Baranger, M. General impact theory of pressure broadening. *Phys. Rev.*, 1958, **112**, 855–865. https://doi.org/10.1103/PhysRev.112.855
25. Mahmoudi, W. F., Ben Nessib, N., and Dimitrijević, M. S. Stark broadening parameters of the singly ionized sulfur: S II. *Adv. Space Res.*, 2023, **71**, 1281–1286. https://doi.org/10.1016/j.asr.2023.01.028
26. Harmon, R. S., Russo, R. E., and Hark, R. R. Applications of laser-induced breakdown spectroscopy for geochemical and environmental analysis: A comprehensive review. *Spectrochim. Acta B*, 2013, **87**, 11–26. https://doi.org/10.1016/j.sab.2013.05.007